JOURNAL OF PROTEOMICS XX (2011) XXX–XXX

available at www.sciencedirect.com

ScienceDirect

www.elsevier.com/locate/jprot

Shotgun proteomic analysis of the unicellular alga *Ostreococcus tauri*

Thierry Le Bihan[a,*], *Sarah F. Martin*[a], *Eliane S. Chirnside*[a], *Gerben van Ooijen*[a], *Martin E. Barrios-LLerena*[a], *John S. O'Neill*[a,b], *Pavel V. Shliaha*[a], *Lorraine E. Kerr*[a], *Andrew J. Millar*[a]

[a] *Centre for Systems Biology at Edinburgh, The University of Edinburgh, Edinburgh, UK*
[b] *Department of Clinical Neurosciences, University of Cambridge Metabolic Research Laboratories, Institute of Metabolic Science, Cambridge, UK*

ARTICLE INFO

Article history:
Received 10 March 2011
Accepted 17 May 2011

Keywords:
Ostreococcus tauri
Algal proteomics
Label-free quantitation
^{15}N metabolic labeling
Circadian rhythms
Phosphopeptide enrichment

ABSTRACT

Ostreococcus tauri is a unicellular green alga and amongst the smallest and simplest free-living eukaryotes. The *O. tauri* genome sequence was determined in 2006. Molecular, physiological and taxonomic data that has been generated since then highlight its potential as a simple model species for algae and plants. However, its proteome remains largely unexplored. This paper describes the global proteomic study of *O. tauri*, using mass spectrometry-based approaches: phosphopeptide enrichment, cellular fractionation, label-free quantification and ^{15}N metabolic labeling. The *O. tauri* proteome was analyzed under the following conditions: sampling at different times during the circadian cycle, after 24 h of illumination, after 24 h of darkness and under various nitrogen source supply levels. Cell cycle related proteins such as dynamin and kinesin were significantly up-regulated during the daylight-to-darkness transition. This is reflected by their higher intensity at ZT13 and this transition phase coincides with the end of mitosis. Proteins involved in several metabolic mechanisms were found to be up-regulated under low nitrogen conditions, including carbon storage pathways, glycolysis, phosphate transport, and the synthesis of inorganic polyphosphates. *Ostreococcus tauri* responds to low nitrogen conditions by reducing its nitrogen assimilation machinery which suggests an atypical adaptation mechanism for coping with a nutrient-limited environment.

1. Introduction

Algae are a highly diverse and ubiquitous group of eukaryotic photosynthetic organisms that are critical for maintaining atmospheric conditions as they contribute considerably to carbon fixation and oxygen production. Among algae, picophytoplankton are distributed worldwide and play an important role in maintaining coastal ecosystems [1]. *Ostreococcus tauri* is a picoeukaryote which was first identified by Courties in the Thau lagoon in France [2] and has since been found in both coastal waters and in the open ocean [1]. *O. tauri* is the smallest known free-living eukaryote, with a cell diameter of approximately 1 μm. This unicellular organism exhibits one of the simplest ultrastructures, as each cell contains just one chloroplast, one mitochondrion, one Golgi body and one nucleus with one or two nuclear pores [3]. *O. tauri* lacks a structured cell wall and a flagellum or other motility structures. Taxonomically, *O. tauri* belongs to the prasinophytes, a group of green algae at the very base of the kingdom of Viridiplantae, the phylogenetic branch that includes land

* *Corresponding author at:* Centre for Systems Biology at Edinburgh, The University of Edinburgh, School of Biological Sciences, C.H. Waddington Building, The Kings Buildings, Mayfield Road, Edinburgh, UK, EH9 3JD. Tel.: +44 131 651 9073; fax: +44 131 651 9068.
E-mail address: thierry.lebihan@ed.ac.uk (T. Le Bihan).

1874-3919/$ – see front matter © 2011 Elsevier B.V. All rights reserved.
doi:10.1016/j.jprot.2011.05.028

plants. This ancient phylogenetic position implies that studies on the *O. tauri* genome and proteome highlight early stages in the evolutionary development of the green plant lineage. Its minimal cell structure, combined with a high growth rate, makes *O. tauri* an attractive picoeukaryotic green plant model organism [1] well suited to study regulation of the carbon/nitrogen/phosphorus balance and how this impacts metabolism.

The genome of *O. tauri* has been sequenced [4] and found to be 12.5 to 13.0 Mbp. This is significantly smaller than other unicellular green algae such as *Chlamydomonas reinhardtii* at 120 Mbp or land plants like *Arabidopsis* at 125 Mbp. The *O. tauri* genome sequence revealed several unique features including a high level of heterogeneity with two atypical chromosomes, and a very compact genome [4–6]. An unusually primitive light harvesting system was identified, and enzymes involved in the more elaborate C4 photosynthesis were reported. Another unusual feature of *O. tauri* is its high number of 26 potential selenocysteine-containing proteins, a number that is comparable to that found in humans [7]. Despite the extensive genetic characterization, little is known of the biology and physiology of *O. tauri*. Preliminary studies on *O. tauri* have investigated the effects of growth conditions [8] and the timing of cell division [9,10]. Recently, the cryptochrome system [11], the starch division [12], lipid metabolism [13], the circadian clock [14–16] and the light harvesting system for the photosystem I [17] have been studied.

The work presented here describes the development of a range of techniques to enable analyses of the *O. tauri* proteome by liquid-chromatography mass-spectrometry-based proteomics (LC-MS). A rigorous cell harvesting protocol for precise temporal analysis of the proteome was developed, along with an organelle enrichment protocol for plastid (chloroplast and mitochondria), cytoplasm, and nuclei, to facilitate the functional characterization of differentially localized proteins. Phosphopeptide enrichment experiments were performed, resulting in the identification of large numbers of phosphorylated proteins. We present and discuss LC-MS based quantification platforms including both label-free and ^{15}N metabolic labeling strategies, whereby incorporation levels below 98% give rise to challenging analysis as well as an increase in the ambiguity associated with peptide identifications [18].

Finally, we report the first large-scale proteomic analysis of *O. tauri* and present data on differential expression in selected sets of environmental conditions. This study provides global insights into the biology and physiology of *O. tauri*. Whilst the methods developed for these studies and presented in this work allow future more targeted proteomic work on the *O. tauri* model, the resulting lists of proteins described in this global study will be of wide ranging interest in plant science as this model system provides a snapshot of early green cell evolution.

2. Materials and methods

2.1. Materials

All chemicals were purchased from Sigma-Aldrich (UK) unless otherwise stated. Acetonitrile and water for LC-MSMS and sample preparation were HPLC quality (Fisher, UK). Formic acid was Suprapure 98–100% (Merck, Darmstadt, Germany) and trifluoroacetic acid was 99% purity sequencing grade. The stable isotope ^{15}N sodium nitrate (98% purity according to the supplier) and ammonium chloride (99% purity according to the supplier) were purchased from Cambridge Isotope Laboratories. Sequencing grade modified porcine trypsin was purchased from Promega (UK). All HPLC-MS connector fittings were from Upchurch Scientific or Valco (Hichrom and RESTEK, UK). LC-MS buffer constituents are expressed in volume to volume percentages.

2.2. *O. tauri* strain and culturing

O. tauri OTTH0595 [2] was cultured in 0.22 μm filter sterilized artificial sea water (Instant Ocean powder) at a salinity of 30 ppt, supplemented with either commercially available Keller salts or with basic constituents hereof. A complete list of media components and concentrations needed to grow *O. tauri* can be found in supplementary material Table S1 with the addition of an antibiotic cocktail as performed in the study of Farinas et al. [10]. For metabolic labeling studies, Keller salts were prepared from basic constituents, with ^{14}N and ^{15}N from nitrate and ammonium as the only change to exclude effects arising from media differences. Due to the autotrophic nature of *O. tauri*, the only source of nitrogen used in this study was the ammonium and nitrate salt as detailed in supplementary material Table S1. Unless otherwise stated, cells were cultured under a 12 hour daylight/12 hour darkness cycle at a constant 20 °C in a vertical environmental test chamber (MLR-350, Sanyo). A light intensity of 17.5 $\mu Em^2\ s^{-1}$ with a blue filter Ocean Blue, Lee lighting filter 724 was used in all experiments. Cell density was evaluated by measuring the optical density (OD) at 600 nm in parallel with FACS (Fluorescence Activated Cell Sorting) analysis, and total protein was assayed using a Bradford kit (Biorad, UK).

For some experiments, cells were harvested at specific times in the daily cycle, expressed in Zeitgeber Time (ZT), where ZT0 corresponds to dawn. Therefore the specific time point ZT1 corresponds to an hour into the "day", ZT13 to an hour into the "night" and ZT6 and ZT18 are intermediate times. For different nitrogen concentration experiments, *O. tauri* cells were cultured under physiological (9.2×10^{-4} M NO_3 and NH_4 composed of 8.83×10^{-4}M $NaNO_3$ and 3.63×10^{-5}M NH_4Cl) and lower nitrogen conditions (0.5×10^{-4} M NO_3 and NH_4 composed of 4.8×10^{-5}M $NaNO_3$ and 1.97×10^{-6}M NH_4Cl) conditions for 7 days prior to harvesting which was performed at ZT1 and analyzed (see Table S2 for detail). Quantitative analysis of the sampling at 4 time points during the day was performed on biological triplicate samples of the non-soluble/nuclear fraction. Quantitative experiments performed under high and low nitrogen supply conditions were the results from two and three biological replicate samples. All other label-free LC-MS analyses (e.g. plastid and cytoplasm-enriched fractions characterized at different time of the day, under 24 h day and dark samples, the ^{15}N labeling and phosphopeptide enrichment analyses) were performed on one to four biological replicates and are presented in the overview of supplementary Table S2.

Please cite this article as: Le Bihan T, et al, Shotgun proteomic analysis of the unicellular alga *Ostreococcus tauri*, J Prot (2011), doi:10.1016/j.jprot.2011.05.028

2.3. Harvesting cells and organelle enrichment

Cultures were centrifuged (3220 *g*, 10 min, 4 °C) and the resulting pellets were washed with a Phosphate buffered saline solution, PBS (137 mM NaCl, 2.7 mM KCl, 8.1 mM Na_2HPO_4, 1.76 mM KH_2PO_4). For total cell lysate, *O. tauri* cells were lysed in a TissueLyser (Qiagen) at 30 Hz for 3 min, using a ball bearing in a microcentrifuge tube and digested as described below. For organelle fractionation, a pellet from 100 ml culture was resuspended in 200 μl PBS, and then diluted with 800 μL PBS with 0.03% Triton X-100, EDTA-Free protease inhibitor (Roche, UK), and phosphatase inhibitor cocktail 1 and 2. The suspension was homogenized using a Dounce homogenizer, and centrifuged (3220 *g*, 10 min, 4 °C). The supernatant (supernatant 1) was removed and processed to produce plastid- (chloroplasts and mitochondria) and cytoplasm-enriched fractions. The pellet (pellet 1) was washed to create a non-soluble/nuclear-enriched fraction.

Plastid enrichment was achieved by centrifuging supernatant 1 (20000 *g*, 10 min, 4 °C) and carefully removing this cytoplasm-enriched supernatant (supernatant 2). The plastid-enriched pellet was washed once with PBS. The cytoplasm-enriched fraction, supernatant 2 was centrifuged (3220 *g*, 20 min, 4 °C) on a 3 kDa cut-off membrane (Vivaspin, Sartorius Stedim), the upper solution was reconstituted with 200 μL PBS, and re-centrifuged (3220 *g*, 40 min, 4 °C). The later step was repeated once, before the resulting upper layer solution was used as a cytoplasm-enriched fraction.

To refine the non-soluble/nuclear-enriched fraction, pellet 1 was reconstituted in 1.5 mL PBS containing 1% Triton X-100, homogenized using a Dounce homogenizer, and centrifuged (3220 g, 10 min, 4 °C). This step was repeated and the pellet was rinsed with PBS and centrifuged (6000 *g*, 5 min, 4 °C) to obtain the non-soluble protein/nuclear-enriched fraction. All extraction procedures were performed on ice and cells were lysed within 20 min of harvesting in all cases.

2.4. Digest and peptide clean-up

Protein samples were diluted in water to 300 μl. After adding 125 μl 8 M Urea, 25 μl 1 M ammonium bicarbonate, and 25 μl 200 mM dithiothreithol, samples were incubated for 30 min at RT to enable denaturation and reduction followed by cysteine alkylation with 25 μl 500 mM iodoacetamide. Trypsin digest was performed overnight by adding 10 μg trypsin. 10 μl of the digested solution was cleaned using Stagetips [19].

2.5. Phosphopeptide enrichment

Titanium columns (4 cm × 400 μm) were packed with Titansphere 10 μm media. Columns were conditioned with 200 μl 80% acetonitrile containing 0.1% TFA. Peptide samples (200 μg) were reconstituted in 50 μl solution 1 (0.1% formic acid, 2.5% acetonitrile) and 50 μl solution 2 (80% acetonitrile, 0.1% TFA, 200 mg/mL 2,5-dihydroxy-benzoic acid) and loaded on the columns at 3–5 μl/min. Columns were subsequently washed with 200 μl solution 2, and 400 μl 80% acetonitrile containing 0.1% TFA. Phosphopeptides were eluted in the following 3 steps: First elution: 30 μl solution 3 (70 mM ammonia pH 10). Second elution: 40 μl solution 3 plus 10 μl 7 N ammonium hydroxide. Third elution: 40 μl acetonitrile plus 10 μl 7 N ammonium hydroxide. The 3 eluates were pooled, dried, and stored at −20 °C.

2.6. HPLC and mass spectrometry for proteomics analysis

Capillary-HPLC-MSMS analysis was performed on an on-line system consisting of a micro-pump (1200 binary HPLC system, Agilent, UK) coupled to a hybrid LTQ-Orbitrap XL instrument (Thermo-Fisher, UK). The LTQ was controlled through Xcalibur 2.0.7. HPLC-MS methods have been described previously [20]. Samples were reconstituted in 10 μl loading buffer before injection, and analyzed on a 2 hour gradient for data dependent analysis.

2.7. Data processing

Conversion from RAW to MGF files was performed as described previously [20]. MSMS data were searched using MASCOT Versions 2.2 and 2.3 (Matrix Science Ltd, UK) against the *O. tauri* subset of the NCBI protein database (March 2008) using a maximum missed-cut value of 2. Variable methionine oxidation, STY phosphorylation, protein N-terminal acetylation and fixed cysteine carbamidomethylation were used in all searches. Precursor mass tolerance was set to 7 ppm and MSMS tolerance to 0.4 amu. The significance threshold (p) was set below 0.05 (MudPIT scoring). Groups of experiments were combined using Maxquant (version 1.0.13.8), assuming a false positive rate of 0.01 [21]. To analyse ^{15}N incorporation, Maxquant was used to cluster proteins based on the detection of the natural isotope. ^{15}N metabolic labeling was analyzed using Mascot 2.2 and 2.3 in combination with Mascot Distiller version 2.3.2.0. LC-MS label-free quantification was performed using Progenesis 2.6 (Nonlinear Dynamics, UK).

For label free quantitation, the number of Features (i.e. signal at a specific retention time and m/z) was reduced to only MSMS peaks with a charge of 2, 3, or 4+ and only the five most intense MSMS spectra per "Feature" were kept. Sets of multicharged ions (2+,3+,4+) were extracted from each LC-MS run and their intensities summed for normalization purposes. Protein quantitation was performed as follows; for a given protein, the associated peptide ion intensities detected in the samples were summed (favoring the more reliable higher abundant ions) to generate an abundance value which is representative of a protein in each sample. From the measured protein abundances, the within group means were calculated to determine the fold change and this data was used to calculate the *p* values by one way ANOVA. Differentially expressed proteins were considered meaningful under the following conditions: Only proteins detected by two or more peptides, with an absolute ratio of at least 2 and *p* values <0.05 associated with the protein change.

To quantify ^{15}N metabolic labeling, only 95% and 98% incorporation levels were considered (detailed in the Results and Discussion Section 3.2 Response to aberrant photoperiods) assuming co-elution of both light and heavy peptides.

Please cite this article as: Le Bihan T, et al, Shotgun proteomic analysis of the unicellular alga *Ostreococcus tauri*, J Prot (2011), doi:10.1016/j.jprot.2011.05.028

Protein ratios were determined from the median peptides ratio (Light:Heavy) with peptide thresholds set to "at least homology". The level of ^{15}N incorporation was determined using a high throughput tool that will be described elsewhere (S. F. Martin, unpublished data). Briefly, a list of peptides and retention time are extracted from a Mascot output from a non labeled identification experiment. From the labeled LC-MS run, centroid MS peaks are extracted in function of time using ReADW.exe (http://sourceforge.net/projects/sashimi/). For each peptide, MS isotope peaks are extracted at predicted masses (+/−12 ppm) for the complete ^{15}N labeling range. The mass prediction is based on the MS-Isotope approximation (http://prospector.ucsf.edu/). Scans were averaged over the MSMS trigger time +/−15 s. The extracted peaks from are then fitted by simulating the ^{15}N incorporation in 0.5% steps and the best least squares fit is kept.

Peptide MSMS fragmentation assignments were prepared by combining Mascot output and Protein Prospector (http://prospector.ucsf.edu/). Protein localization was evaluated using PSORT [22] and similarity search performed using BLAST at NCBI (http://blast.ncbi.nlm.nih.gov/). Data were converted using the Pride converter v2.4.2 [23] and are available on the public data repository PRIDE (http://www.ebi.ac.uk/pride/).

3. Results and discussion

To quantify differential expression in the *O. tauri* proteome, robust sampling and organelle fractionation procedures were combined with mass spectrometry-based proteomics strategies. By analysing the organism under a variety of different experimental conditions, 2343 proteins were identified across all experiments (1794 proteins with 2 peptides and more). There are a total of 8565 proteins reported in *O. tauri* proteome so this corresponds to 27% coverage of the proteome (21% with ≥2 peptides). A complete description of the experiments is presented in supplementary material Table S2 and lists of identified proteins (based on MaxQuant output) are provided in supplementary Table S3. In summary, 53 LC-MS label-free runs identified 2115 proteins of which 1679 were represented by two or more peptides. In 48 LC-MS $^{15}N/^{14}N$ metabolic labeling runs, a total of 1454 proteins were identified (1100 by two or more peptides) and in 20 runs with phosphopeptide-enriched samples, over 573 phosphopeptides with a Mascot score of ≥20 were identified.

The protein profiles of cell fractions were used to produce a Venn diagram (Fig. 1A) to illustrate the separation of proteins and the number of unique proteins within each fraction (proteins identified with at least 2 peptides or more in a given run). This illustrates that although a relatively simple fractionation procedure was used (not employing ultracentrifugation), three distinct pools of proteins were produced.

The Use of PSORT for organelle prediction localization on the proteins found in each fraction is shown in Fig. 1B. Proteins predicted to be located in the plastid (mitrochondria and chloroplast combined) are dominating all 3 fractions. However, the nuclear enriched fraction contains the higher portion of predicted nuclear proteins and the cytoplasm enriched fraction contains the higher portion of predicted cytoplasmic proteins. Regarding the plastid fraction, the ratio plastid/total protein is at its highest in the plastid fraction. The fact that all fractions seem to contain predominantly plastid proteins according to PSORT could be due to a combination of both an experimental contaminations as well as an overestimation by PSORT of the number of proteins having a plastid localization in the case of *O. tauri*.

In supplementary information, Table S4 reports the list of proteins found in the different fractions and the PSORT prediction is presented for each protein.

We have highlighted a few examples of different scenarios with an emphasis toward a nuclear localization. Several transcription factors such as DEAD-box protein abstract gi|116059391|, Transcriptional activator gi|116000610|, myc-regulated gi|116059626| and the nuclear localization sequence binding protein gi|116059177| were found uniquely in the nuclear fraction which was also confirmed with high PSORT score for a nuclear localization. However, other proteins were also found mostly exclusively in the nuclear fraction such as chromatin-remodeling complex ATPase ISWI2 gi|116058982| as well as SAR DNA-binding protein-1 gi|116056427| and the nucleolar RNA-associated family protein gi|116058956| which in all cases PSORT predicted a localization to the cytoplasm. Finally, the protein SYNO_ARATH Asparaginyl-tRNA synthetase, chloroplast/mitochondrial precursor gi|116061103| was also predicted to be localized by PSORT in the chloroplast/mitochondria, however, was mainly found in the cytoplasm.

We are aware that selecting a small set of proteins to demonstrate the quality of the fractionation on one hand and PSORT reliability on the other is biased. For this reason we have shown examples that cover each instance.

3.1. *Differential protein expression in the 24 hour cycle*

Circadian rhythms are endogenous biological programs that anticipate the solar cycle and orchestrate important metabolic and physiological events to the most appropriate time of day. In higher plants, it has been reported that as much as a third of the transcriptome is circadian regulated [24,25]. Tight circadian regulation of the cell cycle has been demonstrated in *O. tauri*[15]. Gene expression during *O. tauri* cell and circadian cycles have been analyzed using stably-transformed luciferase reporter lines [14–16,26]. Several studies on circadian effects have also been performed on other algae, including *Chlamydomonas reinhardtii* [27,28].

Based on sequence homology with other organisms, potential proteins involved in the circadian clock were identified in the *O. tauri* proteome. Kinases and phosphatases fulfill an essential role in circadian control [29] and low abundance phosphorylated proteins that were detected after phosphopeptide enrichment, included seven proteins with a possible function in circadian orchestration (Table 1). The trends in phosphorylation patterns were not significant.

To identify time-of-day specific changes in the proteome that relate to timed processes like the cell cycle or starch synthesis, cells were cultured under a diurnal cycle of 12 h of

Please cite this article as: Le Bihan T, et al, Shotgun proteomic analysis of the unicellular alga *Ostreococcus tauri*, J Prot (2011), doi:10.1016/j.jprot.2011.05.028

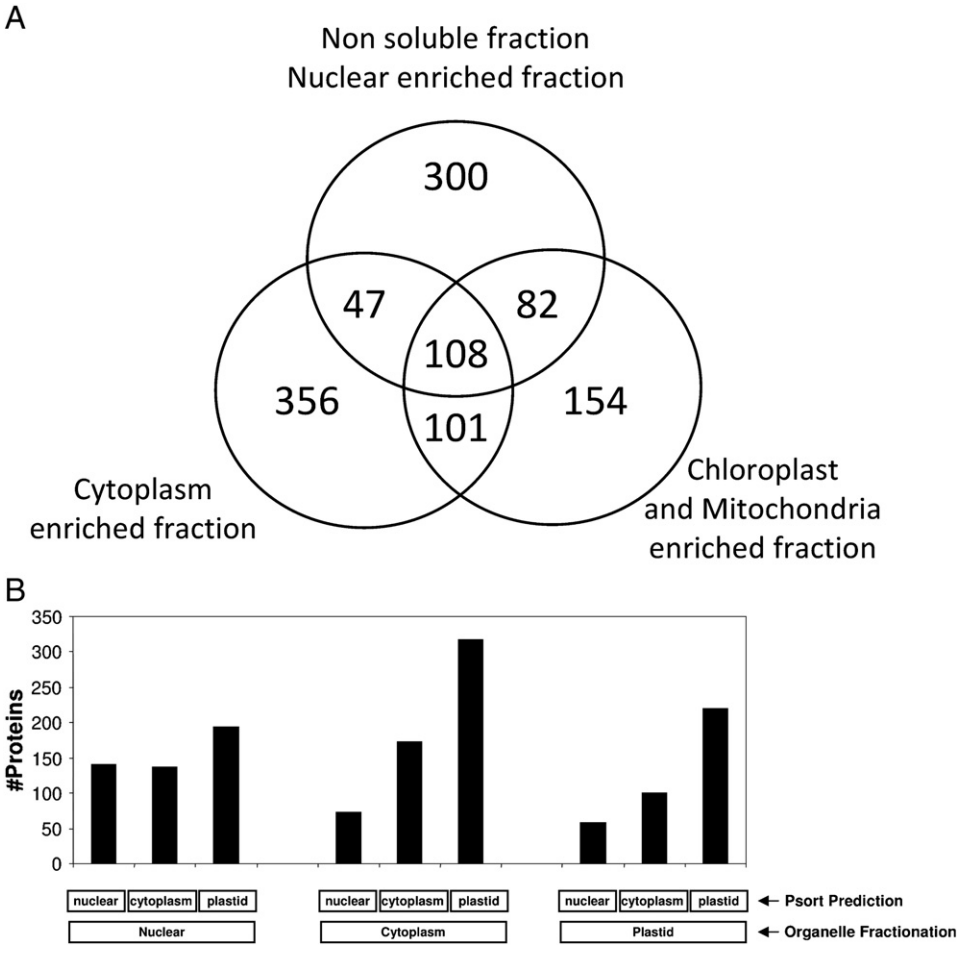

Fig. 1 – A) Venn diagram showing groups of unique and common proteins identified in 21 LC-MS runs of non-soluble/nuclear-, plastid- and cytoplasm-enriched fractions at ZT1, ZT6, ZT13 and ZT18 and data from cells grown under nitrogen sufficient condition identified with at least 2 peptides per protein in a given run. B) PSORT prediction output performed on each fraction. All data are presented in Supplementary Table S4.

daylight and 12 h of darkness. Cells were harvested at specific times of in the daily cycle, expressed in zeitgeber time (ZT), where ZT0 corresponds to dawn. Non-soluble/nuclear-enriched fractions of samples taken at ZT1, ZT6, ZT13 and ZT18 were analysed under label-free conditions and normalized intensities are shown in Fig. 2. Interestingly, cell cycle related proteins like dynamin and kinesin, were significantly up-regulated at the day-to-dark transition as reflected by higher intensity at ZT13 (Fig. 2A,D). This phasing coincides with the end of the strictly timed mitosis [15]. Dynamin has been shown to have a role in membrane remodeling during cytokinesis/mitosis [30] and also kinesin, a microtubule motor, plays a crucial role in mitosis [31]. Other changes in protein expression over time included a significant change in

Table 1 – Phosphopeptides identified from a set of proteins known to be involved in the circadian clock.

Pos.	ID	Proteins description	# Sites [a]	Amino acid [b]	Mascot score	Modified sequence	z	m/z	Δmass [ppm]
146	gi|116057353|	CONSTANS	1	S	47	DEPFGGDVHDGIDTS(ph)SPR	2	990.902	-0.34
395	-	-	1	S	27	VSS(ph)VPDLSK	2	506.242	0.12
961	gi|116057578|	Cryptochrome 1	1	S	62	ATTGSEVS(ph)PAVSGR	2	699.817	-0.42
412	gi|116059668|	PAS	1	S	45	SYS(ph)AGSLAATQK	2	632.284	-0.09
102	gi|51948334|	LHY	1	S	54	EQIVASGSEGS(ph)GSTR	2	772.833	0.19
105	gi|51948340|	APRR	1	S	60	S(ph)ETNAVAAAGEDGGER	2	807.326	-0.29
353	gi|116061773|	Casein kinase I	1	T	26	RQT(ph)TLER	2	492.237	-0.10
210	gi|116057022|	GSK3	1	Y	72	ILAPTEPNISY(ph)ICSR	2	907.431	0.06

[a] Number of amino acids predicted to be phosphorylated
[b] Predicted phosphorylated amino acids

Please cite this article as: Le Bihan T, et al, Shotgun proteomic analysis of the unicellular alga *Ostreococcus tauri*, J Prot (2011), doi:10.1016/j.jprot.2011.05.028

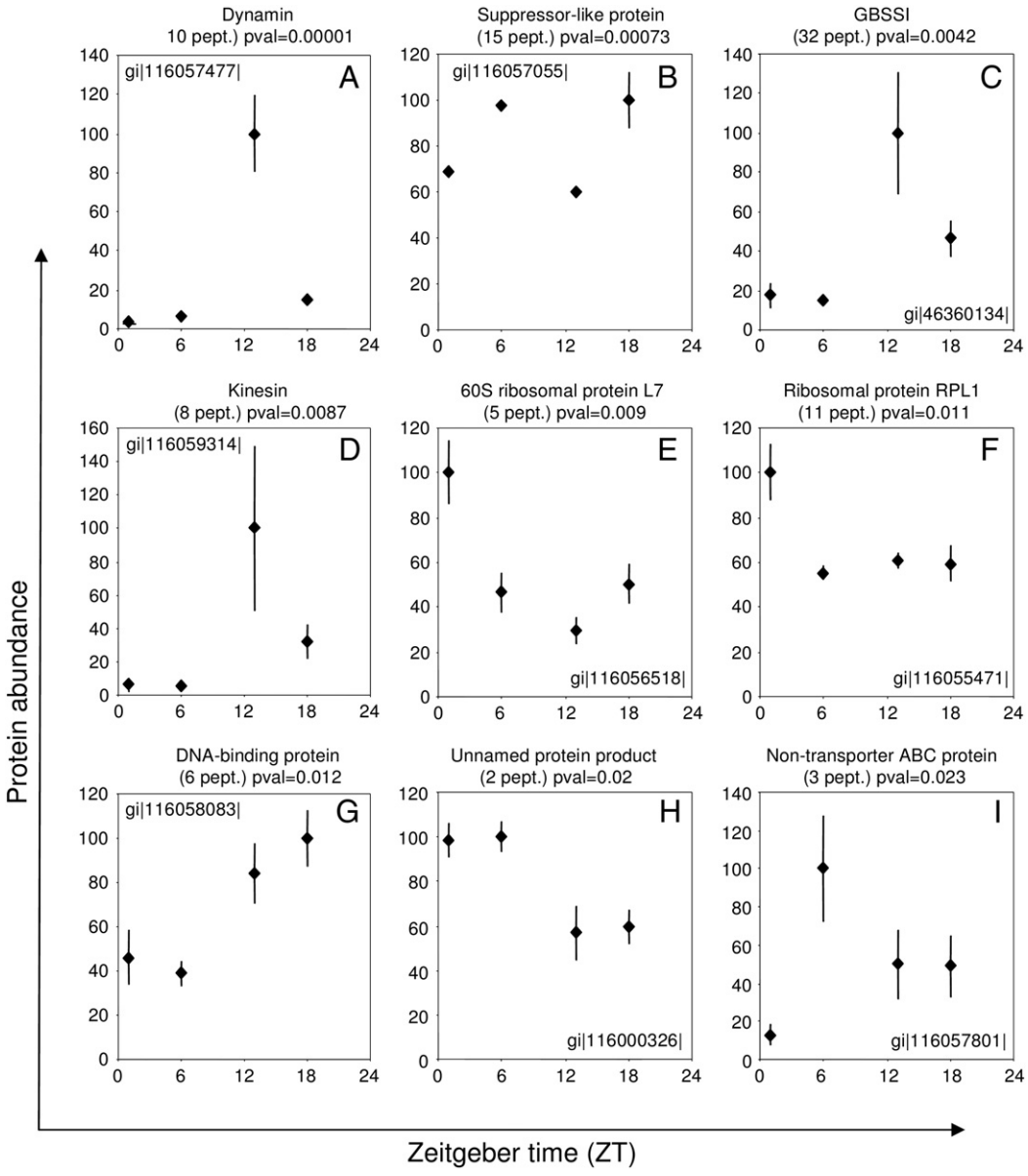

Fig. 2 – Combined normalized intensities from triplicate experiments of protein abundance identified and quantified on the non-soluble /nuclear enriched fraction with a label free quantitative analysis performed at ZT1, ZT6, ZT13, and ZT18 with at least 2 peptides and *p* value lower than 0.03 (see Material and methods for the label free quantitation details). A complete list of the proteins identified under circadian regulation is presented in Supplementary Table S5.

Granule-Bound Starch Synthase I (GBSSI). Abundance of GBSSI in the non-soluble/nuclear-enriched pellet probably reflects accumulation in starch particles. GBSSI expression increases during the day to reach a peak in the early night (Fig. 2C), which is similar to the expression pattern of its *Chlamydomonas* homolog [28]. These results demonstrate that proteins up-regulated at different times can be identified by the methods described in this paper. The complete label-free MS quantitative analysis performed using Progenesis on circadian regulation of protein expression is presented in Supplementary Table S5.

3.2. *Response to aberrant photoperiods*

As discussed above, the cell cycle is tightly clock regulated, and the clock is entrained by external cues such as day/dark transitions arising from the diurnal cycle. Substantial perturbation of the physiologically normal cycle could shed light on some of the mechanisms underlying the orchestration of this timing. In other words, measuring expression patterns after extending the day or the night with 12 h (resulting in 24 h day or 24 h dark) enables the distinction between innate circadially regulated timed oscillations and acute responses to day

Please cite this article as: Le Bihan T, et al, Shotgun proteomic analysis of the unicellular alga *Ostreococcus tauri*, J Prot (2011), doi:10.1016/j.jprot.2011.05.028

or darkness. For example, starch content in *Chlamydomonas reinhardtii* oscillates even in constant darkness, suggesting that this is a clock-regulated system [28]. However, in the unicellular alga *Guillardia theta*, this free-running behaviour is not observed, and an evening-phased day-dark transition has been shown to be essential to trigger starch synthesis [32].

Differentially treated *O. tauri* cultures were grown in media containing either ^{14}N or ^{15}N, and pooled at equal densities at harvest for metabolic labeling experiments. Using this ^{15}N metabolic quantitation approach, we compared the level of GBSSI after 24 h day (LL) or 24 h of darkness (DD) (Fig. 3). Prior to this 24 h shift, *O. tauri* was grown under alternating 12 h day/dark cycles. To a certain extent, these experimental conditions allow for the discrimination between events occurring due to external illumination cue and the control of the endogenous clock since the time at which cells were harvested corresponds to subjective dusk (ZT12) for DD and subjective dawn (ZT0) for LL. The level of GBSSI decreased below the detection limit after 24 h of darkness, suggesting that starch synthesis in *O. tauri* is directly following the day cycle and is potentially triggered by day-to-dark transitions rather than oscillating under tight circadian regulation. This result is confirmed by reciprocal ^{15}N metabolic labeling (result not shown).

In addition to GBSSI, the expression dynamics of Late Elongated Hypocotyl (LHY, gi|51948334|) was interrogated with ^{15}N metabolic labeling. LHY is a morning-phased MYB-like transcription factor and an important component of the circadian clock component in *Arabidopsis thaliana*[33]. Importantly, the LHY peptide previously identified by phospho-enrichment (Table 1) was more abundant in the LL samples than in the DD samples (Fig. 4) which is in line with its circadially timed peak expression time around dawn. This result verifies that a protein expected to be under tight regulation of the clock did not show direct responses to aberrant light input.

Analysis tools for metabolic labeling assume either complete, or a known, fixed level of stable isotope incorporation. The level of ^{15}N incorporation determined from a pool of 200 peptides was estimated at a median of 95.5±2%. This deviation can lead to distorted quantification, as exemplified using a peptide from photosystem I subunit V (gi|116057633| as shown in Fig. 5. ^{14}N (L) and ^{15}N (H) samples were grown under identical conditions and pooled in a 1 to 1 ratio. Assuming 98% ^{15}N incorporation, the analysis returns a L/H ratio of 1.6. At a set 95% incorporation, the ratio is 1.07, which is closer to the expected 1:1. Estimation of the ^{15}N incorporation level is necessary for each peptide to allow exact metabolic

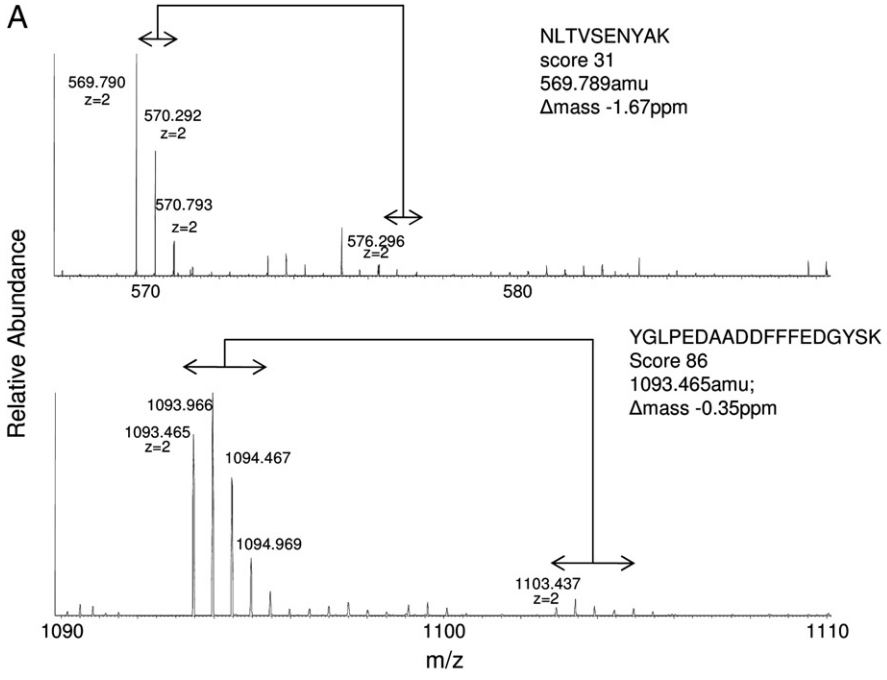

B

Sequence	Mass	Δmass ppm	score	z	L/H	Std.Err.	Correlation	Intensity
NLTVSENYAK	569.7896	-1.67	31	2	18.39	0.09272	0.9989	5.70E+05
GCDIMFEAVPK	633.7964	-0.07	37	2	19.49	0.2536	0.9874	1.15E+05
IFVDHPDFLAK	651.3472	-1.29	50	2	18.37	0.4891	0.9959	2.41E+05
LDAAEPNCAGVVK	672.3348	0.03	40	2	28.63	0.2452	0.9935	5.49E+05
AVPNAQVVILGTGK	683.905	-1.92	44	2	20.04	0.224	0.9989	5.16E+05
IVFVSAECSPWSK	755.3737	-0.31	74	2	24.29	0.1875	0.9972	3.41E+05
YGLPEDAADDFFFEDGYSK	1093.4651	-0.35	86	2	16.05	0.1107	0.9994	4.31E+05
QALQAEVGLPLDPTAPVFGYIGR	1206.6487	-0.86	72	2	17.75	0.1448	0.9986	2.16E+05
QALQAEVGLPLDPTAPVFGYIGR	804.7687	-0.21	32	3	23.05	0.179	0.9995	3.26E+05

Fig. 3 – A) Quantification of a peptide derived from GBSSI (NLTVSENYAK) using ^{15}N metabolic labeling after 24 h darkness (DD) or 24 h light (LL, ^{14}N) assuming 95% ^{15}N incorporation. B) Global quantitation of GBSSI-derived peptides using Mascot Distiller.

Please cite this article as: Le Bihan T, et al, Shotgun proteomic analysis of the unicellular alga *Ostreococcus tauri*, J Prot (2011), doi:10.1016/j.jprot.2011.05.028

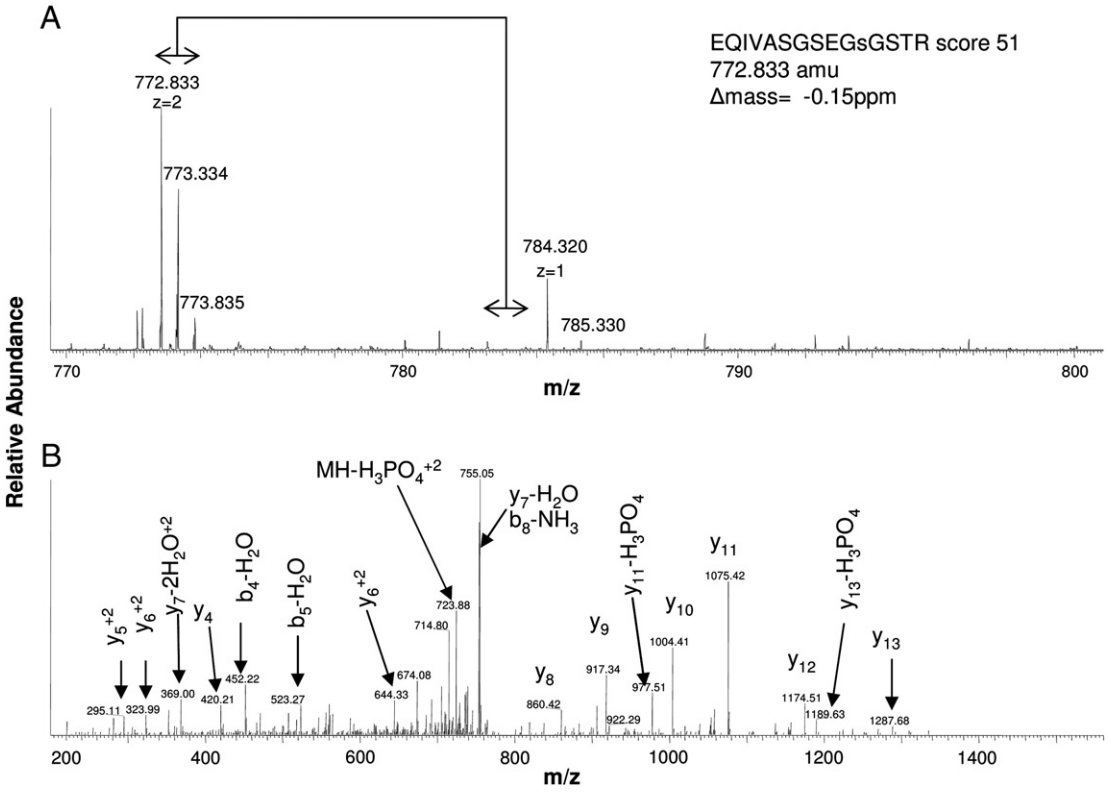

Fig. 4 – A) Quantification of a phosphorylated peptide derived from LHY using ^{15}N metabolic labeling in 24 h light (LL, ^{14}N) that is not present after 24 h darkness (DD, ^{15}N) assuming 95% ^{15}N incorporation. B) Collision-induced fragmentation ion spectra of the LHY phosphopeptide and details of the major detected fragments.

quantitation. However we found that using a fixed average value is adequate for a semi-quantitative evaluation and provides robust results as described above. For applications that require higher accuracy, further development of quantitative analysis tools, able to deal with partial labeling over a range of different incorporation ratios are required.

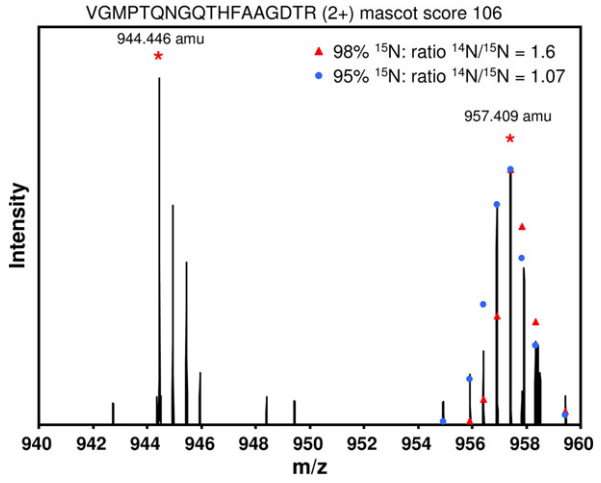

Fig. 5 – MS spectrum for a peptide (VGMPTQNGQTHFAAGDTR) derived from photosystem I subunit V, with mass difference resulting from ^{14}N or ^{15}N labeling. Stars highlight the ^{12}C ^{14}N component and the ^{12}C ^{15}N component of the same peptide. Triangles indicate peaks used for ratio calculation assuming 98% ^{15}N incorporation and circles those used for an assumed 95% ^{15}N incorporation.

3.3. *O. tauri under low nitrogen supply*

Nutrient acquisition strategies, especially for nitrogen, are essential to survive, particularly in the restrictive (oligotrophic) marine environment. The high surface-to-volume ratio resulting from its small size combined with its high number of ammonium transporter genes makes *O. tauri* a strong competitor for nitrogen resources [4] and an interesting model to investigate efficient nitrogen assimilation in eukaryotes. Using flow cytometric analysis, *O. tauri* growth under low nitrogen conditions and carbon uptake has previously been studied [8], revealing a strong initial adaptation to nutrient stress, suggesting a quick global alteration of metabolism. A number of metabolic studies have been carried out on nitrogen deprived plants and algae, focused on specific enzymes involved in carbon and nitrogen assimilation and amino acid synthesis [34–36]. In contrast to these focused studies, a global, non hypothesis driven proteomic approach would generate an extensive list of proteins that have not yet been directly linked to nitrogen deprivation responses, and *O. tauri* is a highly suitable organism for such a study. A similar approach was undertaken by Wegener et al. 2010 on the prokaryote cyanobacterium *Synechocystis* [37].

Please cite this article as: Le Bihan T, et al, Shotgun proteomic analysis of the unicellular alga *Ostreococcus tauri*, J Prot (2011), doi:10.1016/j.jprot.2011.05.028

O. tauri cells were cultured under either physiological or low nitrogen conditions for 7 days. Label-free analysis of changes in the proteome was performed on cellular fractions (Supplementary information Table S6A is the non-soluble/nuclear-enriched fraction; Table S6B is the plastid-enriched fraction; and Table S6C is the cytoplasm-enriched fraction). Under lower nitrogen conditions, ribosomal proteins and several histones were expressed at lower levels than under physiological conditions (Supp. Table S6A), and several proteins involved in phosphate transport or synthesis of inorganic phosphates were up-regulated in the non-soluble/nuclear-enriched fraction (Supp. Table S6A). These include polyphosphate kinase, ATP carrier protein nucleotide transporter, GTP binding protein, Pho4 high affinity phosphate transporter and the AtpB ATP synthase. This result is in line with the previously described accumulation of inorganic polyphosphate under nitrogen deprivation in *Chlorella* [38]. Proteins involved in glycolysis were also up-regulated under low nitrogen conditions, including phosphoglycerate kinase, chloroplast glyceraldehyde-3-phosphate dehydrogenase subunits A and B, and glucose-6-phosphate-1-dehydrogenase. Interestingly, starch accumulation proteins, including GBSSI, were also up-regulated in low nitrogen-conditions, as well as proteins involved in fatty acid oxidation and methionine synthesis (Supp. Table S6A). Although the expression of high affinity phosphate transporters is mostly induced under phosphate-limiting conditions [39], the Pho4 transporter was also found to be up-regulated in all three fractions of the cells grown under low nitrogen source.

Surprisingly, in the plastid and cytoplasmic-enriched fraction, several proteins involved in nitrogen assimilation (urea high-affinity symporter, and proteins related to nitrate high-affinity transporters) were found to be down-regulated (expressed as ratio low nitrogen/normal nitrogen conditions in Supp. Table S6B and C). Such a behavior is in contrast to what has been reported for other models such as *Arabidopsis thaliana*[40] or in alga *Chlorella sorokiniana* [41]. The down-regulation of proteins involved in nitrogen assimilation under lower nitrogen conditions although counter-intuitive has also been observed previously in *Prochlorococcus* a marine photosynthetic prokaryote [42]. El Alaoui et al. 2003 [42] present an elegant explanation regarding this behavior and this atypical response could be associated to an adaptation by both *Ostreococcus* and *Prochlorococcus* for surviving under oligotrophic conditions (i.e. under low nitrogen conditions in this case). Both avoid the production of expensive proteins involved into the nitrogen assimilation pathway when there is limited nitrogen to assimilate. This adaptation could represent a selective advantage during a long term continued nitrogen depletion in the marine environment. This behavior distinguishes *O. tauri* from higher organisms.

The combination of the information obtained from three protein fractions in low nitrogen conditions revealed up-regulation of proteins involved in carbohydrate storage, including GBSSI, ADP-glucose-pyrophosphorylase (AGPSU1), starch phosphorylase 3, and UDP-glucose 4 epimerase. A similar group of proteins has been found to be up-regulated in the common bean (*Phaseolus vulgaris*) in response to storage protein deficiency [43]. AGPSU1 has been previously shown to play a crucial role in carbon accumulation directed to starch formation in preference to the synthesis of triacylglycerol [44]. Proteins involved in the pentose pathway and glycolysis were also up-regulated as were proteins involved in the glycolysis pathway and ER secretory pathway.

Global expression patterns of the majority of proteins show a coordinated regulation across the three organelle fractions under any given condition. However, two proteins revealed a divergent trend: Rbcl (gi|112806877|) was up-regulated in the non-soluble/nuclear-enriched fraction (ratio low nitrogen/normal nitrogen conditions), but was down-regulated (ratio low nitrogen/normal nitrogen conditions) in the cytoplasm-enriched fraction. A similar profile was identified for myosin class II heavy chain (gi|116057101|). In both conditions, the same ratio of chloroplast-based proteins was found using PSORT, ruling out preferential enrichment of chloroplast proteins in the non-soluble fraction under low nitrogen conditions. In addition to Rbcl and myosin, several other proteins also found to be up-regulated in the non-soluble fraction are proteins potentially associated to phagosome (such as, calnexin, clathrin, GTP binding protein) [45]. One possible explanation is that *O. tauri* mobilizes nitrogen from abundant proteins under low nitrogen conditions in a similar mechanism as that described in higher plants [46] or in yeast [47].

Twelve percent of proteins demonstrating a higher expression under physiological conditions were proteins with currently unknown functions. In contrast, under low nitrogen conditions, almost 50% of the total proteins that were up-regulated in the chloroplast and mitochondrion-enriched fraction were unknown proteins. This discrepancy might simply reflect that most research is carried out under non-stressed conditions, but some of these proteins of unknown functions might be involved in the adaptation mechanism to nitrogen deprivation.

4. Concluding remarks

In this study, we present the first global proteomic analysis of *O. tauri*. A robust cell harvesting protocol and an organelle enrichment workflow to isolate non-soluble/nuclear-, plastid- and cytoplasm-enriched fractions are reported, alongside a set of culture techniques. Phosphopeptide enrichment, label-free quantification and ^{15}N quantitation were applied and the experimental issues associated with the different approaches discussed. Specific observations include that starch synthase GBSSI did not display clock-driven oscillations but follows day/dark cues. For the latter, follow-up experiments using an exogenous source of carbon will undoubtedly clarify GBSSI dependency toward either a circadian or a light trigger event. Proteins involved in glycolysis were up-regulated under low nitrogen conditions, as well as other metabolic pathways including carbon storage, phosphate transport, and the synthesis of inorganic polyphosphates. Sugar accumulation could potentially shut down photosynthetic activity under low nitrogen conditions, and we hypothesize those abundant proteins like Rubisco could serve as an alternative source of nitrogen through autophagy. This seems plausible since a number of proteins that are involved in autophagy have been

Please cite this article as: Le Bihan T, et al, Shotgun proteomic analysis of the unicellular alga *Ostreococcus tauri*, J Prot (2011), doi:10.1016/j.jprot.2011.05.028

shown to be up-regulated in response to low nitrogen conditions [48]. In parallel, some of the data presented here suggests that *O. tauri* exhibits some similarity to *Prochlorococcus* with regards to adaptation mechanisms in the nitrogen assimilation pathway which could have a crucial function in its capability to adapt and survive under conditions of nutrient restriction. In more general terms, this study introduces a range of technical developments that will enable follow-up proteomic studies using *O. tauri* as a model species for accelerated research into higher organisms.

Supplementary materials related to this article can be found online at doi:10.1016/j.jprot.2011.05.028.

Acknowledgements

TLB, SFM, ESC, MBL, GvO, JON, LEK and AJM are funded by the Centre for Systems Biology at Edinburgh (CSBE) which is a Centre for Integrative Systems Biology (CISB) funded by BBSRC and EPSRC; reference BB/D019621/1.

REFERENCES

[1] Archibald JM. Genome complexity in a lean, mean photosynthetic machine. Proc Natl Acad Sci USA 2006;103(31):11433–4.
[2] Courties C, Vaquer A, Trousselier M, Lautier J, Chrétiennot-Dinet MJ, Neveux J, et al. Smallest eukarotic organism. Nature 1994;370:255.
[3] Henderson GP, Gan L, Jensen GJ. 3-D ultrastructure of *O. tauri*: electron cryotomography of an entire eukaryotic cell. PLoS One 2007;2(8):e749, doi:10.1371/journal.pone.0000749.
[4] Derelle E, Ferraz C, Rombauts S, Rouzé P, Worden AZ, Robbens S, et al. Genome analysis of the smallest free-living eukaryote *Ostreococcus tauri* unveils many unique features. Proc Natl Acad Sci USA 2006;103(31):11647–52.
[5] Misumi O, Yoshida Y, Nishida K, Fujiwara T, Sakajiri T, Hirooka S, et al. Genome analysis and its significance in four unicellular algae, *Cyanidioshyzon merolae*, *Ostreococcus tauri*, *Chlamydomonas reinhardtii*, and *Thalassiosira pseudonana*. J Plant Res 2008;121:3–17.
[6] Keeling PJ. *Ostreococcus tauri*: seeing through the genes to the genome. Trends Genet 2007;23(4):151–4.
[7] Lobanov AV, Fomenko DE, Zhang Y, Sengupta A, Hatfield DL, Gladyshev VN. Evolutionary dynamics of eukaryotic selenoproteomes: large selenoproteomes may associate with aquatic life and small with terrestrial life. Genome Biol 2007;8(9):R198.
[8] Fouilland E, Descolas-Gros C, Courties C, Collos Y, Vaquer A, Gasc A. Productivity and growth of a natural population of the smallest free-living eukaryote under nitrogen deficiency and sufficiency. Microb Ecol 2004;48(1):103–10.
[9] Khadaroo B, Robbens S, Ferraz C, Derelle E, Ferraz C, Inzé D, et al. The first green lineage cdc25 dual-specificity phosphatase. Cell Cycle 2004;3(4):513–8.
[10] Farinas B, Mary C, de O Manes CL, Bhaud Y, Peaucellier G, Moreau H. Natural synchronisation for the study of cell division in the green unicellular alga *Ostreococcus tauri*. Plant Mol Biol 2006;60(2):277–92.
[11] Heijde M, Zabulon G, Corellou F, Ishikawa T, Brazard J, Usman A, et al. Characterization of two members of the Cryptochrome/Photolyase family from *Ostreococcus tauri* provides insights into the origin and evolution of cryptochromes. Plant Cell Environ 2010;33(10):1614–26.
[12] Ral JP, Derelle E, Ferraz C, Wattebled F, Farinas B, Corellou F, et al. Starch division and partitioning. A mechanism for granule propagation and maintenance in the picophytoplanktonic green alga *Ostreococcus tauri*. Plant Physiol 2004;136(2):3333–40.
[13] Wagner M, Hoppe K, Czabany T, Heilmann M, Daum G, Feussner I, et al. Identification and characterization of an acyl-CoA: diacylglycerol acyltransferase 2 (DGAT2) gene from the microalga *O. tauri*. Plant Physiol Biochem 2010;48(6):407–16.
[14] Djouani-Tahri el B, Motta JP, Bouget FY, Corellou F. Insights into the regulation of the core clock component TOC1 in the green picoeukaryote *Ostreococcus*. Plant Signal Behav 2010;5(3):332–5.
[15] Monnier A, Liverani S, Bouvet R, Jesson B, Smith JQ, Mosser J, et al. Orchestrated transcription of biological processes in the marine picoeukaryote *Ostreococcus* exposed to light/dark cycles. BMC Genomics 2010;11:192 PMID: 20307298.
[16] Corellou F, Schwartz C, Motta JP, Djouani-Tahri el B, Sanchez F, Bouget FY. Clocks in the green lineage: comparative functional analysis of the circadian architecture of the picoeukaryote ostreococcus. Plant Cell 2009;21(11):3436–49.
[17] Swingley WD, Iwai M, Chen Y, Ozawa SI, Takizawa K, Takahashi Y, et al. Characterization of photosystem I antenna proteins in the prasinophyte *Ostreococcus tauri*. Biochim Biophys Acta 2010;1797(8):1458–64.
[18] Nelson CJ, Huttlin EL, Hegeman AD, Harms AC, Sussman MR. Implications of ^{15}N-metabolic labeling for automated peptide identification in *Arabidopsis thaliana*. Proteomics 2007;7(8):1279–92.
[19] Rappsilber J, Mann M, Ishihama Y. Protocol for micro-purification, enrichment, pre-fractionation and storage of peptides for proteomics using StageTips. Nat Protoc 2007;2(8):1896–906.
[20] Le Bihan T, Grima R, Martin SF, Forster T, Le Bihan Y. Quantitative analysis of low-abundance peptides in HeLa cell cytoplasm by targeted liquid chromatography/mass spectrometry and stable isotope dilution: emphasising the distinction between peptide detection and peptide identification. Rapid Commun Mass Spectrom 2010;24(7):1093–104.
[21] Cox J, Matic I, Hilger M, Nagaraj N, Selbach M, Olsen JV, et al. A practical guide to the MaxQuant computational platform for SILAC-based quantitative proteomics. Nat Protoc 2009;4(5):698–705.
[22] Horton P, Park KJ, Obayashi T, Fujita N, Harada H, Adams-Collier CJ, et al. WoLF PSORT: protein localization predictor. Nucleic Acids Res 2007(35 (Web Server issue)):W585–7.
[23] Barsnes H, Vizcaíno JA, Eidhammer I, Martens L. PRIDE Converter: making proteomics data-sharing easy. Nat Biotechnol 2009;27(7):598–9.
[24] Carré IA, Kim JY. MYB transcription factors in the Arabidopsis circadian clock. J Exp Bot 2002;53(374):1551–7.
[25] Smith KM, Sancar G, Dekhang R, Sullivan CM, et al. Transcription factors in light and circadian clock signaling networks revealed by genome-wide mapping of direct targets for *Neurospora* white collar complex. Eukaryot Cell 2010;9(10):1549–56.
[26] Corellou F, Camasses A, Ligat L, Peaucellier G, Bouget FY. Atypical regulation of a green lineage-specific B-type cyclin-dependent kinase. Plant Physiol 2005;138(3):1627–36.
[27] Mittag M, Kiaulehn S, Johnson CH. The circadian clock in *Chlamydomonas reinhardtii*. What is it for? what is it similar to? Plant Physiol 2005;137:399–409.
[28] Ral JP, Colleoni C, Wattebled F, Dauvillée D, Nempont C, Deschamps P, et al. Circadian clock regulation of starch metabolism establishes GBSSI as a major contributor to amylopectin synthesis in *Chlamydomonas reinhardtii*. Plant Physiol 2006;142(1):305–17.
[29] Hirota T, Lewis WG, Liu AC, Lee JW, Schultz PG, Kay SA. A chemical biology approach reveals period shortening of the mammalian circadian clock by specific inhibition of GSK-3beta. Proc Natl Acad Sci USA 2008;105(52):20746–51.

[30] Bonner MK, Skop AR. Cell division screens and dynamin. Biochem Soc Trans 2008;36(3):431–5.
[31] Tomishige M. Activation of mitotic kinesin by microtubule bundling. J Cell Biol 2008;182(3):417–9.
[32] Haferkamp I, Deschamps P, Ast M, Jeblick W, Maier U, Ball S, et al. Molecular and biochemical analysis of periplastidial starch metabolism in the cryptophyte *Guillardia theta*. Eukaryot Cell 2006;5(6):964–71.
[33] Alabadí D, Oyama T, Yanovsky MJ, Harmon FG, Más P, Kay SA. Reciprocal regulation between TOC1 and LHY/CCA1 within the *Arabidopsis* circadian clock. Science 2001;293(5531):880–3.
[34] Richardson B, Orcutt DM, Schwertner HA, Martinez CL, Wickline HE. Effects of nitrogen limitation on the growth and composition of unicellular algae in continuous culture. Appl Microbiol 1969;18(2):245–50.
[35] Zhila NO, Kalacheva GS, Volova TG. Influence of nitrogen deficiency on biochemical composition of the green alga *Botryococcus*. J of Applied Phycology 2005;17:309–15.
[36] Huppe HC, Turpin DH. Integration of carbon and nitrogen metabolism in plant and algal cells. Annu Rev Plant Physiol Plant Mol Biol 1994;45:577–607.
[37] Wegener KM, Singh AK, Jacobs JM, Elvitigala T, Welsh EA, Keren N, et al. Global proteomics reveal an atypical strategy for carbon/nitrogen assimilation by a cyanobacterium under diverse environmental perturbations. Mol Cell Proteomics 2010;9(12):2678–89.
[38] Kuesel AC, Sianoudis J, Leibfritz D, Grimme LH, Mayer A. P-31 in-vivo NMR investigation on the function of polyphosphates as phosphate- and energy source during the regreening of the green alga *Chlorella fusca*. Arch Microbiol 1989;152:167–71.
[39] Persson BL, Petersson J, Fristedt U, Weinander R, Berhe A, Pattison J. Phosphate permeases of *Saccharomyces cerevisiae*: structure, function and regulation. Biochim Biophys Acta 1999;1422(3): 255–72.
[40] Lemaître T, Gaufichon L, Boutet-Mercey S, Christ A, Masclaux-Daubresse C. Enzymatic and metabolic diagnostic of nitrogen deficiency in *Arabidopsis thaliana* Wassileskija accession. Plant Cell Physiol 2008;49(7):1056–65.
[41] Tischner R, Huttermann A. Regulation of glutamine synthetase by light and during nitrogen deficiency in synchronous *Chlorella sorokiniana*. Plant Physiol 1980;66:805–8.
[42] El Alaoui S, Diez J, Toribio F, Gómez-Baena G, Dufresne A, García-Fernández JM. Glutamine synthetase from the marine cyanobacteria *Prochlorococcus* spp characterization, phylogeny and response to nutrient limitation. Environ Microbiol 2003;5 (5):412–23.
[43] Marsolais F, Pajak A, Yin F, Taylor M, Gabriel M, Merino DM, et al. Proteomic analysis of common bean seed with storage protein deficiency reveals up-regulation of sulfur-rich proteins and starch and raffinose metabolic enzymes, and down-regulation of the secretory pathway. J Proteomics 2010;73(8):1587–600.
[44] Li Y, Han D, Hu G, Dauvillee D, Sommerfeld M, Ball S, et al. *Chlamydomonas* starchless mutant defective in ADP-glucose pyrophosphorylase hyper-accumulates triacylglycerol. Metab Eng 2010;12(4): 387–91.
[45] Shui W, Sheu L, Liu J, Smart B, Petzold CJ, Hsieh TY, et al. Membrane proteomics of phagosomes suggests a connection to autophagy. Proc Natl Acad Sci USA 2008;105 (44):16952–7.
[46] Ishida H, Yoshimoto K, Izumi M, Reisen D, Ohsumi Y, Mae T, et al. Mobilization of rubisco and stroma-localized fluorescent proteins of chloroplasts to the vacuole by an ATG gene-dependent autophagic process. Plant Physiol 2008;148 (1):142–55.
[47] Kolkman A, Daran-Lapujade P, Fullaondo A, Olsthoorn MM, Pronk JT, Slijper M, et al. Proteome analysis of yeast response to various nutrient limitations. Mol Syst Biol 2006;2 2006.0026.
[48] Yorimitsu T, Klionsky DJ. Eating the endoplasmic reticulum: quality control by autophagy. Trend in Cell Biol 2007;17(6): 279–85.

Please cite this article as: Le Bihan T, et al, Shotgun proteomic analysis of the unicellular alga *Ostreococcus tauri*, J Prot (2011), doi:10.1016/j.jprot.2011.05.028